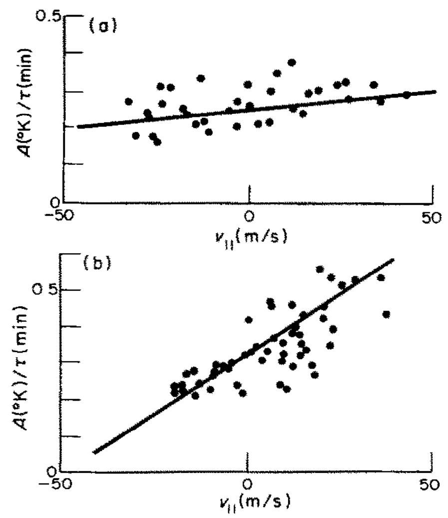

FIG. 1. THE VALUES OF A/τ VS $V_{||}$.

We believe that the next eleven cases can be regarded as a result of the passage of waves from a monochromatic source of internal gravitational waves, a source situated in a small region. In this case the wave with a definite period will only pass through the base triangle vertex the distance of which to the source satisfies ratio 1. In the other four cases these waves were not recorded at all since this ratio apparently was not fulfilled for any vertex of the base triangle.

These results are an argument in favour of the conclusion that some regions of the jet stream over active meteorological formations were the sources of the internal gravitational waves observed by the hydroxyl emission. The establishment of the mechanism of their selective excitation will be the subject of further studies.

We wish to express gratitude to Academician A. M. Oboukhov for attention to our work without which these investigations could not have been carried out.

V. I. Krassovsky
M. V. Shagaev

Institute of the Physics of the Atmosphere,
USSR Academy of Sciences,
Moscow,
USSR

REFERENCES

Krassovsky, V. I. (1972). Infrasonic variations of OH emission in the upper atmosphere. *Ann. Géophys.* **28**, 739.

Krassovsky, V. I. and Shagaev, M. V. (1974a). Optical method of recording acoustic or gravity waves in the upper atmosphere. *J. atmos. terr. Phys.* **36**, 373.

Krassovsky, V. I. and Shagaev, M. V. (1974b). Inhomogeneities and wavelike variations of the rotational temperature of atmospheric hydroxyl. *Planet. Space Sci.* **22**, 1334.

Krassovsky, V. I., Kuzmin, K. I., Piterskaya, N. A., Semenov, A. I., Shagaev, M. V., Shefov, N. N. and Toroshelidze, T. I. (1975). Results of some airglow observations of internal gravitational waves. *Planet. Space Sci.* **23**, 896.

Hines, C. O. (1968). A possible source of waves in noctilucent clouds. *J. atmos. Sci.* **25**, 937.

Planet. Space Sci., Vol. 25, pp. 201 to 203. Pergamon Press, 1977. Printed in Northern Ireland

FITTING OF HYDRODYNAMIC AND KINETIC SOLAR WIND MODELS

(*Received* 23 *August* 1976)

Abstract—In isothermal models of the expanding solar corona there exists in general an exobase level where the collision mean free path becomes equal to the density scale height. At this level the hydrodynamic approximations of the transport equations fail to be justified and a kinetic approach is more appropriate. This exobase is located below the altitude of the critical point proper to the hydrodynamic solutions. The bulk velocity at the exobase is subsonic and smaller than the expansion velocity at the critical point. Therefore the transition to a supersonic solar wind velocity occurs in the collisionless ion-exosphere.

Despite the early success of the hydrodynamic models to predict supersonic flow velocities and the observed densities at 1 a.u. in the solar wind, it is now widely accepted that the general plasma transport equations can be closed up only in the *collision dominated* region of the corona (i.e. for $r < 5$–$10\ R_S$). Indeed, the heat flux and stresses are limited there by Coulomb collisions and the Chapman–Enskog approximations are fully applicable. At larger radial distances from the Sun, however, a kinetic or exospheric approach is more appropriate. The purpose of this note is to show that it is generally possible to fit kinetic solutions and hydrodynamic solutions through an exobase interface where the Knudsen number of the plasma is equal to unity. The requirement that the density and particle flux (and eventually higher order moments of the particles velocity distribution) are continuous across

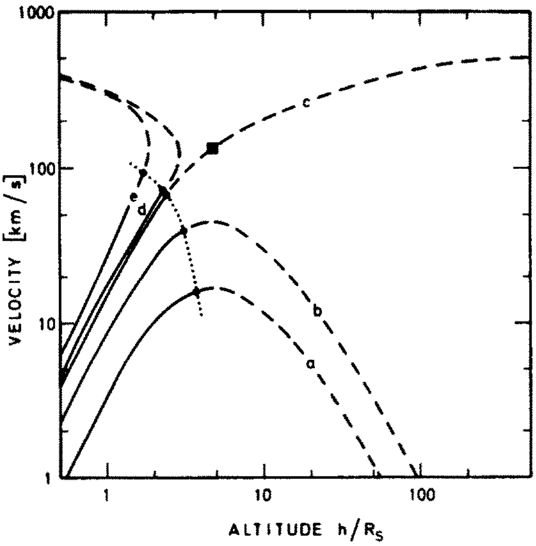

FIG. 1. SOLAR WIND FLOW VELOCITIES.

The solid and dashed curves refer to hydrodynamic isothermal models for which $T_e = T_p = 10^6$ K; at $h_0 = 0.5\, R_S$ (a) $w_0 = 0.8$ km/s; (b) $w_0 = 2.15$ km/s; (c) $w_0 = (w_0)_c = 3.996$ km/s; (d) $w_0 = 4.5$ km/s; (e) $w_0 = 7.6$ km/s. The solid dots indicate for each of these five models the exobase altitude (h_{exb}) and flow speed (w_{exb}). The solid square corresponds to the critical point of the hydrodynamic Euler equations.

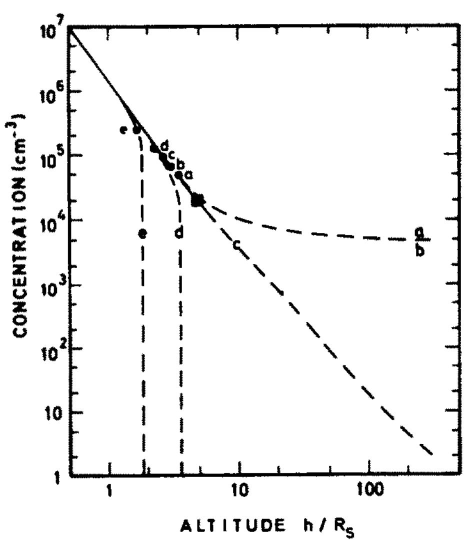

FIG. 2. SOLAR WIND DENSITIES.

The solid and dashed curves refer to hydrodynamic isothermal models for which $T_e = T_p = 10^6$ K; at $h_0 = 0.5\, R_S$ $n_0 = 10^7$ cm^{-3} and (a) $w_0 = 0.8$ km/s; (b) $w_0 = 2.15$ km/s; (c) $w_0 = (w_0)_c = 3.996$ km/s; (d) $w_0 = 4.5$ km/s; (e) $w_0 = 7.6$ km/s. The solid dots indicate for each of these five models the exobase altitude (h_{exb}) and density (n_{exb}); the solid square corresponds to the critical point of the hydrodynamic Euler equations.

the exobase surface determines uniquely a hydrodynamic solution which is, in general, different from the "critical solution" passing through the "critical point". The critical point is located at a higher altitude than the exobase. As a consequence a kinetic approximation can be used (instead of the hydrodynamic approximations) to describe the transition from the subsonic to the supersonic flow regime.

The solid and dashed curves in Figs. 1 and 2 are distributions of flow speed (w) and densities (n) for five different hydrodynamic isothermal models ($T_e = T_p = 10^6$ K). At the reference altitude ($h_0 = 0.5\, R_S : R_S$ is the Sun Radius), the densities of the protons and electrons are the same in all the models considered ($n_0 = 10^7$ cm^{-3}), but the flow speeds are respectively given by: (a) $w_0 = 0.8$ km/s; (b) $w_0 = 2.15$ km/s; (c) $w_0 = (w_0)_c = 3.996$ km/s; (d) $w_0 = 4.5$ km/s; (e) $w_0 = 7.6$ km/s; $(w_0)_c$ corresponds to the critical model c passing through the critical point (h_c, w_c) where $h_c = (GMm_p/4kT_p) - R_S$ and $w_c = (2kT_p/m_p)^{1/2}$.

At large radial distances, the density of the subsonic models a and b tends to a constant value (n_∞) which is unreasonably large compared to 5–10 cm^{-3} observed at 1 a.u. (Parker, 1963).

In the "super critical" models d and e the density (n) and the density scale height ($H = |dh/d \ln n|$) drop rapidly to zero near $h = 3.5\, R_S$ and $h = 1.7\, R_S$, respectively.

On the other hand, the mean free path of a proton with thermal velocity [$v = (8kT_p/\pi m_p)^{1/2}$] is given by:

$$\bar{l} = 7200 \frac{T_p^2}{n} \text{ [in cm]},$$

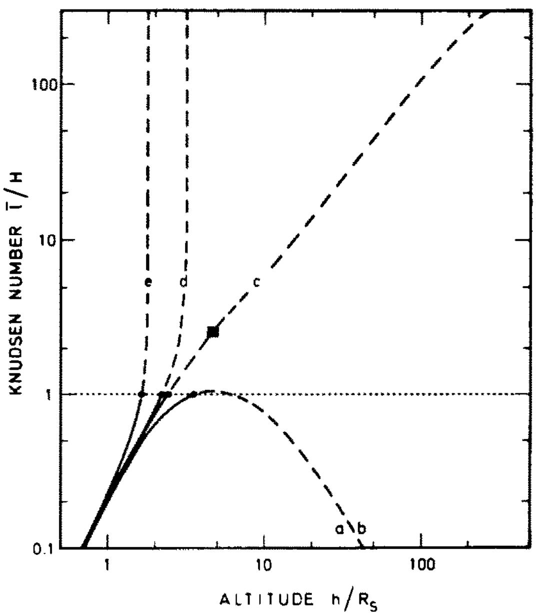

FIG. 3. KNUDSEN NUMBERS IN THE SOLAR WIND.

The solid and dashed curves refer to the five hydrodynamic models illustrated in Figs. 1 and 2. The solid dots indicate the exobase altitudes (h_{exb}) where the mean free path becomes equal to the density scale height. Note that the exobase is below the critical point altitude for all the "supercritical" solutions.

(T_p in K; n in cm^{-3}) (Spitzer, 1956). The value of $\bar{l}$ depends on the altitude in each of the five hydrodynamic models considered. This is illustrated in Fig. 3 where the solid and dashed curves correspond to the ratio $\bar{l}/H$ (i.e. the local Knudsen Number) in the five hydrodynamic models. The exobase is generally defined as the altitude where $\bar{l}/H = 1$ (indicated by solid dots in Figs. 1, 2 and 3). It can be seen that for all "super critical" hydrodynamic models [i.e. for $w_0 > (w_0)_c$] the exobase is *below* the critical point altitude ($h_{exb} < h_c$). Furthermore, the flow speed at the exobase is *smaller* than the critical velocity or the local thermal velocity ($w_{exb} < w_c = (2kT_p/m_p)^{1/2}$). Therefore the critical point is situated in a region of the corona where the local Knudsen Number of the plasma is larger than unity, i.e. in the ion-exosphere where the hydrodynamic or Chapman–Enskog approximations are no longer appropriate. Kinetic models like those described by Jockers (1970) and Lemaire and Scherer (1971) can be constructed to join up the hydrodynamic models *d* and *e*. Indeed it is possible to build kinetic models which have a given exobase density (n_{exb}), a given particle flux ($n_{exb}w_{exb}$) or any value for higher order moments of the velocity distribution of the particles (Lemaire and Scherer 1971, 1973). As a consequence it is possible to fit kinetic solutions with hydrodynamic solutions by imposing continuity of density, particle flux, and other higher order moments across the exobase interface. Conversely, it is possible to adjust a hydrodynamic solution (e.g. by fitting $w_0 \ldots$) to join up with a given kinetic solution which satisfactorily describes the solar wind at 1 a.u.

G. Brasseur
J. Lemaire

Institut d'Aeronomie Spatiale,
3 avenue Circulaire,
B-1180 Brussels,
Belgium

REFERENCES

Jockers, K. (1970). Solar wind models based on exospheric theory. *Astron. Astrophys.* **6**, 219.
Lemaire, J. and Scherer, M. (1973). Kinetic models of the Solar and Polar Winds. *Rev. Geophys. Space Phys.* **11**, 427.
Lemaire, J. and Scherer, M. (1971). Kinetic models of the solar wind. *J. geophys. Res.* **76**, 7479.
Parker, E. M. (1963). *Interplanetary Dynamical Processes,* Interscience, New York.
Spitzer, Jr., L. (1956). *The Physics of Fully Ionized Gases.* Interscience, New York.

Planet. Space Sci., Vol. 25, pp. 203 to 204. Pergamon Press, 1977. Printed in Northern Ireland

ON THE VALIDITY OF THE CHAPMAN–ENSKOG DESCRIPTION OF THE SOLAR WIND

(*Received* 15 *July* 1976)

Abstract—The validity of the Chapman–Enskog method in the calculation of the heat conductivity of the solar wind is studied. The predictions of the Chapman–Enskog theory are compared with known results of rarefied gas kinetic theory. The results suggest that the use of the Chapman–Enskog theory to describe the transport processes in the solar wind is not strictly justified.

In a recent paper, Price, Brandt and Wolff (1975) presented experimental results in support of the use of the Chapman–Enskog (CE) method for the description of the transport processes in the solar wind. The validity of this method and the applicability of the hydrodynamic models for the solar wind have often been discussed (Leer and Holzer, 1972; Hundhausen, 1972; Lemaire and Scherer, 1973). It is an important task to verify whether the application of the CE method to the solar wind is justified. The purpose of this note is to point out that the arguments presented by Price *et al.* (1975) remain inconclusive.

It is useful first to trace briefly through the CE theory for the heat conduction flux for the solar wind protons and derive the result given by equations (8) and (10) in their paper. The calculation is based on the well-known transport theory for a *collision dominated*, neutral, one component gas (Ferziger and Kaper, 1972; Chapman and Cowling, 1952). The distribution function f is assumed expandable in a small nonuniformity parameter ϵ about a local Maxwellian $f^{(0)}$, that is,

$$f = f^{(0)}(1 + \epsilon\psi + \epsilon^2\psi^2 + \ldots). \tag{1}$$

In equation (1), $\phi = \epsilon\psi$ is the departure from local equilibrium to first order in ϵ, where for many applications ϵ can be taken to be the ratio of the mean free path, l, and a convenient macroscopic length parameter. The perturbation ϕ_q, induced by a temperature gradient ∇T is given by

$$\phi_q = -\frac{1}{n}\mathbf{A}\cdot\nabla \ln T \tag{2}$$

where n is the number density and $\mathbf{A}$ satisfies the CE